

# The $H\alpha$ Luminosity Function and Star Formation Rate at $z \sim 0.2$

Laurence Tresse<sup>1</sup> and Steve J. Maddox  
*Institute of Astronomy, Cambridge, CB3 0HA, UK*

## ABSTRACT

We have measured the  $H\alpha + [N II]$  fluxes of the  $I$ -selected Canada–France Redshift Survey (CFRS) galaxies lying at a redshift  $z$  below 0.3, and hence derived the  $H\alpha$  luminosity function. The magnitude limits of the CFRS mean that only the galaxies with  $M_B \gtrsim -21$  mag were observed at these redshifts. We obtained a total  $H\alpha$  luminosity density of at least  $10^{39.44 \pm 0.04} \text{ erg s}^{-1} \text{ Mpc}^{-3}$  at a mean  $z = 0.2$  for galaxies with rest-frame  $EW(H\alpha + [N II]) \gtrsim 10 \text{ \AA}$ . This is twice the value found in the local universe by Gallego et al. 1995. Our  $H\alpha$  star formation rate, derived from Madau (1997) is higher than the UV observations at same  $z$ , implying a UV dust extinction of  $\sim 1$  mag. We found a strong correlation between the  $H\alpha$  luminosity and the absolute magnitude in the  $B$ -band:  $M(B_{AB}) = 46.7 - 1.6 \log L(H\alpha)$ . This work will serve as a basis of future studies of  $H\alpha$  luminosity distributions measured from optically-selected spectroscopic surveys of the distant universe, and it will provide a better understanding of the physical processes responsible for the observed galaxy evolution.

*Subject headings:* galaxies: luminosity function, mass function - galaxies: evolution

Accepted for publication in *Astrophysical Journal*

---

<sup>1</sup>Visiting observer with the Canada-France-Hawaii Telescope, operated by the NRC of Canada, the CNRS of France and the University of Hawaii.

## 1. Introduction

Deep spectroscopic surveys recently lead to a major breakthrough in our understanding of global galaxy evolution. The Canada–France Redshift Survey (CFRS) (Lilly et al. 1995c) clearly demonstrated an evolution in the galaxy population up to a redshift  $z \sim 1$ , which has been confirmed by the Autofib Survey (Ellis et al. 1996). Data combining observations from the Keck Telescope and Hubble Space Telescope (Steidel et al. 1996a) reach the star-forming galaxy population up to  $z \sim 3 - 4$ . Thus, a picture of the star-formation history has emerged from these observations (Madau et al. 1996), suggesting that the peak of star formation is in the range  $z = 1.3 - 2.7$ .

The observed evolution of the galaxy population is closely related to the history of the star-forming galaxies showing spectral emission lines. Careful analysis of their spectra give crucial information about the physical processes occurring in these galaxies (Tresse et al. 1996, Hammer et al. 1997). In the optical wavelength range, the  $H\alpha(\lambda 6563)$  emission-line flux is a direct tracer of recent star formation. Massive, hot, short-lived OB stars emit ultraviolet (UV) photons, that ionize the surrounding gas to form an H II region, where the recombinations produce spectral emission lines. Of the Balmer lines,  $H\alpha$  is the most directly proportional to the ionizing UV stellar spectra at  $\lambda < 912 \text{ \AA}$  (see Osterbrock 1989 for a review), because the weaker Balmer lines are much more affected by the equivalent absorption lines produced in stellar atmospheres. The other commonly observed optical lines such as [N II] $\lambda\lambda 6548, 6583$ , [S II] $\lambda\lambda 6717, 6731$  and [O II] $\lambda 3727$ , [O III] $\lambda\lambda 4959, 5007$  depend strongly on the metal fraction present in the gas. They have higher ionizing potential than the Balmer lines, thus depend also on the hardness of the ionizing stellar spectra. Therefore they represent only indirect tracers of recent star formation.

The major factor that affects measurements of the true  $H\alpha$  emission fluxes is interstellar extinction. If galaxies are observed at high galactic latitudes, extinction due to our own Galaxy is negligible ( $\sim 0.05$  mag), hence most extinction is intrinsic to the observed galaxy. Star formation takes place in highly obscured regions, so extinction corrections introduce a major uncertainty in estimating the star formation rate. However, since optical wavelengths are less obscured than UV wavelengths,  $H\alpha$  should be a fairly good estimator of recent star formation.

One has to keep in mind that in studies where spectra are obtained for the whole galaxy, the  $H\alpha$  flux from OB stars is produced by H II regions which are distributed throughout both the bulge and disk. Thus the observed line flux has been diluted by the whole stellar and interstellar content of the galaxy. Though line flux measurements depend on the content of an individual galaxy, they allow us to compare populations of galaxies at different cosmic epochs, and so quantify the global physical processes of evolution. Also, if an active nucleus is present in the central region of the galaxy, then the  $H\alpha$  flux is not correlated directly to forming stars, but is a mixture of both. Line ratio diagrams can usually separate H II galaxies from active galaxies. However, if the AGN ionizing spectrum is soft, then the stellar ionizing flux can dominate, and it is more difficult to separate them. At  $z < 0.3$ , the number of AGN-like galaxies is roughly 10% of the number of emission-line galaxies (Tresse et al. 1996, Sarajedini et al. 1996), and so the non-stellar component is not dominant in the global  $H\alpha$  luminosity measurements. Nevertheless at larger redshifts, this situation may change if there is a global evolution in the nuclear activity of galaxies.

Overall, measuring  $H\alpha$  fluxes in representative optically-selected galaxy samples at different cosmic epochs is a major step towards the understanding of the evolutionary processes occurring within the galaxy population. The CFRS provides a preliminary sample for studies of recent star formation. Its wavelength range (4500 – 8500  $\text{\AA}$ ) allows the measurement of  $H\alpha$  fluxes in galaxies at  $z \leq 0.3$ . A full description of the survey has been published in Lilly et al. 1995a for the photometry, in Le Fèvre et al. 1995 for the spectroscopy, in Crampton et al. 1995 for its completeness, and in particular the spectral analysis of the low redshift sample is presented in Tresse et al. 1996 (CFRS-XII).

Section 2 describes the flux measurements and the  $H\alpha$  luminosity function. Section 3 discusses the star formation rate at  $z \simeq 0.2$ . Our conclusions are presented in Section 4.

## 2. The $H\alpha$ luminosity function

The CFRS spectroscopic sample at  $z \leq 0.3$  (138 galaxies) is a fair representation of field galaxies with absolute magnitudes  $-22 < M_{BAB} < -14$  mag<sup>1</sup>, and

---

<sup>1</sup>We assumed  $H_0 = 50 \text{ km s}^{-1} \text{ Mpc}^{-1}$  and  $q_0 = 0.5$  throughout the paper.

with  $\langle z \rangle = 0.2086$  (see Figure 1. Also see Section 2 in CFRS-XII for a detailed description). Because of the  $I$ -band ( $\lambda_c = 8320 \text{ \AA}$ ) selection, these galaxies have been selected by light from the old stellar population, rather than on their young stars. Consequently, our sample is less sensitive to galaxies undergoing strong recent star formation than  $B$ - or  $H\alpha$ -selected surveys at low- $z$ . The wide  $I$  band of width  $2000 \text{ \AA}$  does not favour galaxies with strong  $H\alpha$  emission lines.

## 2.1. The emission-line measurements

The spectral resolution is  $40 \text{ \AA}$ . 117 out of the 138 spectra to  $z = 0.3$  exhibit the blended emission line  $H\alpha + [N \text{ II}]\lambda\lambda 6548, 65683$  (hereafter  $H\alpha + [N \text{ II}]$ ). We have measured the integrated fluxes, equivalent widths and the corresponding  $1 \sigma$  errors for 110 blends ( $H\alpha + [N \text{ II}]$ ) with the package SPLOT under IRAF/CL. For 7 spectra, the blended line could not be properly measured, since it was at the edge of the observed spectral window; in our statistical analysis, we considered them as not observed. The  $1 \sigma$  errors in line flux are typically 10%, the detection level ranges from 2.5 to  $100 \sigma$ . Thus these errors are not a significant source of uncertainty in our final estimate of the  $H\alpha$  luminosity function. Rest-frame equivalent widths (REW) are within the range  $5 - 385 \text{ \AA}$ , and the mean is  $48 \text{ \AA}$ . Only 6% out of the  $H\alpha$  emitters have  $REW(H\alpha + [N \text{ II}]) > 100 \text{ \AA}$ . In Figure 2, we show that except for 3  $H\alpha$  emitters, the sample has a detection limit of REW at about  $10 \text{ \AA}$ , and REW measurements are almost all above  $3 \sigma$ . At  $z \gtrsim 0.2$ , the line  $[O \text{ II}]$  can be detected.  $REW([O \text{ II}])$  are in the range  $4 - 94 \text{ \AA}$ , with a mean of  $14 \text{ \AA}$ . The CFRS spectra at  $z \leq 0.3$  are limited in REW by the poor spectral resolution, rather than the S/N of the continuum because they are the result of  $\sim 7$  hours exposure time. The 21 spectra with no detection of ( $H\alpha + [N \text{ II}]$ ) do not always show  $H\alpha$  in absorption, but all of them have the characteristics of absorption-line spectra: strong  $4000 \text{ \AA}$  break, CaH&K,  $H\beta$  in absorption, G-band, MgI and a very red continuum ( $(V - I_{AB}) \geq 1$ ).

## 2.2. The $H\alpha$ flux measurements

To obtain the flux in  $H\alpha$ , we corrected the flux  $f(H\alpha + [N \text{ II}])$  from the contribution of the doublet  $[N \text{ II}]\lambda\lambda 6583/[N \text{ II}]\lambda 6548 \sim 3$ . Using results from a spectral analysis of the Stromlo-APM survey within the same absolute magnitude range as our emission-line galaxies ( $-21 < M_B < -14$ ), we determined values of  $N_2 = 1.33[N \text{ II}]\lambda 6583/H\alpha$  rang-

ing from 0.15 to 0.55 according to the strength of  $REW(H\alpha + [N \text{ II}])$  (Tresse et al. 1998). This method is in agreement with the trend of the average parameters of  $[N \text{ II}]\lambda 6583/H\alpha$ ,  $EW(H\alpha)$ , and  $V - R$  colors of the UCM emission-lines galaxies (Gallego et al. 1996, Tables 1 & 2). Figure 3b shows the values we have taken.

Where possible we estimated the interstellar extinction at  $H\alpha$  using the  $H\alpha/H\beta$  Balmer decrement. However, it is difficult to correct for reddening for all spectra because the  $40 \text{ \AA}$  spectral resolution and stellar absorption mean that  $H\beta$  is not always seen in emission. We were able to measure the  $H\beta$  integrated fluxes for 55 spectra. For those spectra where we could make a  $3 \sigma$  measurement for  $H\beta$  (40 spectra), the extinction  $C$  has been measured in the following way.

$$10^{-C(-0.323)} = \frac{1}{2.86} \frac{f(H\alpha + [N \text{ II}])/(1 + N_2)}{f(H\beta)}$$

The  $H\alpha/H\beta$  intensity ratio (2.86) is for case B recombination with a density of  $100 \text{ cm}^{-3}$ , and a temperature of  $10\,000 \text{ K}$  (Osterbrock 1989).  $[X(H\alpha) - X(H\beta)]/X(H\beta) = -0.323$  is the value given by the extinction law  $X(\lambda)$  taken from Seaton 1979. We point out that although the different extinction laws are different in the UV, they behave similarly in the visible, hence our results are independent of the choice made. For these 40 spectra,  $\langle C \rangle = 0.36$ . For the other 15 spectra with  $H\beta$  in emission, the average  $C$  is 0.82, or 0.50 if a  $2 \text{ \AA}$  stellar absorption is accounted for at  $H\beta$ ; we retained the latter value. For 10 spectra, we could not measure  $H\beta$  because of a sky line near it, and for the 44 remaining,  $H\beta$  is not detected in emission, probably because of stellar absorption. For these 54 spectra, we decided to apply a correction of  $C = 0.45$ , corresponding to a reddening parameter  $A_V = C R/1.47 \simeq 1 \text{ mag}$  ( $R = 3.2$ , Seaton 1979), which is the average value measured by Kennicutt 1992 in nearby emission-line galaxies. We then corrected our  $H\alpha$  fluxes for reddening as follows:

$$\frac{f(H\alpha + [N \text{ II}])}{1 + N_2} 10^{C(1-0.323)}.$$

We note that the final  $H\alpha$  luminosity densities using these reddening corrections are not significantly different to that using an average of  $A_V = 1 \text{ mag}$  for all galaxies.

The  $1''75$  spectral slits of the CFRS did not always contain the whole galaxy. To have consistent

data, we corrected our fluxes by an aperture correction. For this, we integrated the spectral flux in the V band, and transformed it into magnitudes. The spectrophotometric flux calibration across the spectra is generally accurate to better than 10% (see e.g. Figure 9 in Le Fèvre et al. 1995). The V magnitudes from the CFRS imaging are given by  $I_{AB} + (V - I)_{AB}$ , where  $I_{AB}$  is the isophotal magnitude, and  $(V - I)_{AB}$  is the color of the galaxy measured in an aperture of  $3''$ . The aperture correction is  $a = V_{image} - V_{spectrum}$ . For our emission-line galaxies, the values range between 0 and 1.6 mag, with an average of 0.52. The dereddened  $H\alpha$  flux is then aperture corrected to give the final estimate of the  $H\alpha$  fluxes:

$$f(H\alpha) = \frac{f(H\alpha + [N II])}{1 + N_2} 10^{C(1-0.323)} 10^{0.4 a}.$$

Since at  $z \simeq 0.26$   $H\alpha$  falls at the center of our I band (8320 Å), we could check these aperture corrections, as follows. The integrated flux in  $\text{erg s}^{-1} \text{cm}^{-2}$  in the blended line ( $H\alpha + [N II]$ ) can also be computed using the observed  $EW(H\alpha + [N II])$  in Å and the I-band magnitude in  $\text{erg s}^{-1} \text{cm}^{-2} \text{Å}^{-1}$  to estimate the continuum flux such as,

$$f(H\alpha + [N II]) = EW(H\alpha + [N II]) 1.5 \cdot 10^{-9} 10^{-0.4 I_{AB}}.$$

The differences between the two methods are small, of order 13%. They are due to the facts that the color  $(V - I)_{AB}$  should be the one measured in the spectral slit, and not in a  $3''$  aperture; and that the true continuum level at  $H\alpha$  may not be exactly the mean value given by the I-band magnitude. These discrepancies are much smaller than our Poisson errors, so they do not affect our results on the  $H\alpha$  luminosity function. Another point is that according Kennicutt (1983), the  $H\alpha$  nuclear emission (H II region complexes in the inner disk and bulge regions) is, in general, rarely significant in comparison with the  $H\alpha$  emission from the whole galaxy. Hence, our aperture corrections should not overestimate the  $H\alpha$  measurements, even in the cases of starburst nuclei.

Finally, the  $H\alpha$  luminosity in  $\text{erg s}^{-1}$  is given by:

$$L(H\alpha) = 4 \pi (3.086 \cdot 10^{24} d_L)^2 f(H\alpha),$$

where  $f(H\alpha)$  is the integrated flux in  $\text{erg s}^{-1} \text{cm}^{-2}$ ,  $d_L$  is the luminosity distance in Mpc.

### 2.3. Calculation of the $H\alpha$ luminosity function

Figure 4 shows the comoving  $H\alpha$  luminosity density estimated from our raw data, and from the data

after applying each of the corrections described in Section 2. These densities were obtained using the  $V_{max}$  formalism, i.e.,

$$\Phi[\log L(H\alpha)] \Delta \log L(H\alpha) = \sum_i \frac{1}{V_{max}^i}.$$

$V_{max}^i$  is the comoving volume in which galaxy  $i$  can be detected in this I-selected survey ( $17.5 < I_{AB} < 22.5$ ), and the sum is over galaxies with  $H\alpha$  luminosity within the interval  $[\log L(H\alpha) \pm 0.5 \Delta \log L(H\alpha)]$ .

$$V_{max} = \int_{max(z=0, I_{AB}=17.5)}^{min(z=0.3, I_{AB}=22.5)} d_{<}^2 \frac{dr}{dz} \Omega dz,$$

where  $d_{<}^2$  is the angular distance,  $dr$  the comoving distance at  $z$ , and  $\Omega$  is the effective solid angle of the CFRS observations; 5 fields of  $10'^2$  individually weighted by the number of spectroscopic observations out of the photometric observations. We plotted the comoving densities at the barycenter of the  $\log L(H\alpha)$  of the  $N_i$  data belonging to the interval  $[\log L(H\alpha) \pm 0.5 \Delta \log L(H\alpha)]$ . The density error bars are Poisson errors;  $\log(1 \pm 1/\sqrt{N_i})$ . Figure 4 shows also the Schechter (1976) fit to the local  $H\alpha$  luminosity function (LF) measured by Gallego et al. 1995 ( $\alpha = -1.3$ ,  $\phi^* = 10^{-3.2} \text{Mpc}^{-3}$ ,  $L^* = 10^{42.15} \text{erg s}^{-1}$ ).

Note that we used the  $V_{max}$  based on the  $I_{AB}$  magnitudes, since the galaxy selection is based on this measurement. For the lowest REW, our measurements are not absolutely complete, and so we should, in principle, include this effect in our estimates of  $V_{max}$ . In practice, there is a strong correlation between  $L(H\alpha)$  and  $M_B$  (see Figure 5b), which means that  $V_{max}$  should be only slightly smaller in these cases. We expect the difference in  $V_{max}$  to be small, since lines with low REW are observable even at our maximum redshift,  $z = 0.3$ , as can be seen in Figure 3d. An extreme upper limit to this effect can be obtained by artificially setting  $EW(H\alpha + [N II]) = 5 \text{Å}$  (roughly  $+1\sigma$ ), or  $1 \text{Å}$  for our non  $H\alpha$ -emitting galaxies (15% of the sample). Then using the  $I_{AB}$  magnitudes, we can obtain an approximate flux in  $H(\alpha) + [N II]$ , that we also corrected for  $N_2$ , C (taken as 0.45), and aperture as described in Section 2.2. The LF we obtained in both cases is within the Poisson error bars of our actual results. As these 21 galaxies are very red, a small EW does not produce a small  $L(H\alpha)$ , so they do not produce a steeper LF at the faint end. Thus, our estimated LF is quite stable.

We fitted our overall  $H\alpha$  LF in Figure 4d, with a Schechter function, and the best-fitting parameters given by a weighted minimum  $\chi^2$  are  $\alpha = -1.54 \pm 0.08$ ,  $\phi^* = 10^{-3.28 \pm 0.15} \text{ Mpc}^{-3}$ ,  $L^* = 10^{42.50 \pm 0.23} \text{ erg s}^{-1}$ . If we exclude the faintest bin from the fit which contains only four galaxies, we find:

$$\begin{aligned}\alpha &= -1.35 \pm 0.06 \\ \phi^* &= 10^{-2.83 \pm 0.09} \text{ Mpc}^{-3} \\ L^* &= 10^{42.13 \pm 0.13} \text{ erg s}^{-1}\end{aligned}$$

The quoted errors are the formal  $\chi^2$  fit standard deviations, assuming the parameters are uncorrelated. In fact, these three parameters are highly correlated, so the formal errors are not realistic estimates; the difference between these two fits give a realistic estimate of the true errors. Figure 1 shows that at different redshifts, our survey does not sample exactly the same range of absolute magnitudes. In principle, this could affect our LF, so we calculated the  $H\alpha$  LF using only the galaxies at  $0.17 < z < 0.3$ , and  $-18 < M(B_{AB}) < -21$ , i.e. where the data constitute an homogeneous subsample. The result is shown in Figure 5a and we can see that the resulting densities are entirely consistent with our fitted LFs.

Our  $H\alpha$  LF at  $z \leq 0.3$  samples fainter  $H\alpha$  luminosities than the Gallego et al. 1995 LF; their lowest data is above  $\log L(H\alpha) = 40.4 \text{ erg s}^{-1}$ , ours is at  $39.2 \text{ erg s}^{-1}$ . On the other hand, the ( $I_{AB} < 17.5$ ) CFRS limit and ( $z < 0.3$ ) cut lead to a small volume where we sample bright galaxies with  $M_{B_{AB}} < -21$  mag. According to Figure 5b, this corresponds to  $\log L(H\alpha) \gtrsim 42.3 \text{ erg s}^{-1}$  which explains the large statistical error on our brightest  $H\alpha$  luminosity bin. Also our sample contains a larger proportion of emission-line galaxies with  $5 < \text{REW}(H\alpha + [\text{N II}]) < 30 \text{ \AA}$ . This can be seen in comparing Figures 9 & 10 in Gallego et al. 1996, and our Figures 3c and 3d.

Although it may be expected that blue galaxies correspond to star-forming galaxies, Figure 5c shows that there is not a clear correlation between the ( $V - I$ ) color of a galaxy and  $L(H\alpha)$  in our sample. There is however, a trend seen in Figure 5e, implying blue galaxies tend to have higher  $\text{REW}(H\alpha + [\text{N II}])$ . The latter is in agreement with Figure 10 in Kennicutt (1983), which plots  $\text{REW}(H\alpha + [\text{N II}])$  against  $B - V$  colors for a nearby sample of Sa-Irr galaxies. These figures show that  $\text{REW}(H\alpha)$  is sensitive to the ratio of ionizing stars (which produce  $H\alpha$ ) to lower mass

red giant stars (which produce the stellar continuum at  $H\alpha$ ).

On one hand, this means that we have detected red <sup>1</sup> galaxies which show both low and high  $H\alpha$  fluxes, and that these contribute to the overall luminosity as well as the blue galaxies, for which emission lines are easier to detect because of a lower stellar continuum at  $H\alpha$ . Following the terminology in Gallego et al. 1996, these red galaxies are likely to correspond to Starburst Nuclei Galaxies (SBN) if  $H\alpha$  is bright, and to Dwarf Amorphous Nuclear Starbursts (DANS) when  $\log L(H\alpha) < 41.6$ . Both classes are spiral galaxies. According to Tresse et al. 1996 and Gallego et al. 1996, they represent  $\sim 40\%$  of emission-line galaxies, the remaining being spectrally classified as H II galaxies, blue compact galaxies, or active galaxies.

On the other hand, the lack of a correlation between  $H\alpha$  luminosities and continuum colors means that  $H\alpha$  production is independent of the overall stellar content, and depends only on the recent star formation. The observed ( $V - I$ )<sub>AB</sub> at  $0.1 < z < 0.3$  is rest-frame ( $B - R$ )<sub>AB</sub> which may be significantly reddened. However the typical reddening is ( $A_B - A_R$ )  $\sim 0.2$  mag which would not make blue galaxies appear as red as we observe. The independence of  $L(H\alpha)$  on total stellar content can also be seen in the fact that red galaxies classified in class (B) by Tresse et al. 1996 often show spectral features proving the presence of a dominant old stellar population (CaH&K, G-band, MgI; see Figure 1 of Tresse et al. 1996). So, we suspect that some red galaxies show recent star formation similar to blue galaxies.

Figure 5b shows a tight relation between  $H\alpha$  luminosities and  $B$  luminosities, both of which being closely related to recent star formation. A least squares fit gives:

$$M(B_{AB}) = 46.7 - 1.6 \log L(H\alpha).$$

If this relation holds at higher redshifts,  $0.3 < z < 1$ , we would expect that the high- $z$  CFRS galaxies, which are brighter than  $-20$  in  $B$ , should exhibit stronger  $H\alpha$  emission lines than those observed locally. This is in agreement with the results of Hammer et al. 1997 who found a large increase in the comoving  $[\text{O II}]$  luminosities up to  $z \sim 1$  in the CFRS ( $[\text{O II}]$  luminosities being indirectly related to  $H\alpha$  luminosities).

<sup>1</sup>At  $z < 0.3$ , galaxies having ( $V - I$ )<sub>AB</sub>  $\gtrsim 0.7$  are redder than a local Sb spiral (see Figure 13 in Tresse et al. 1996)

### 3. Star Formation rate at $z \simeq 0.2$

We integrated our best-fit luminosity function to give the overall comoving luminosity density at  $\langle z \rangle = 0.2$ :

$$\mathcal{L}(H\alpha) = \int_0^\infty \phi(L) L dL = \phi^* L^* \Gamma(2 + \alpha)$$

We then find a total H $\alpha$  luminosity per unit volume ranging from  $10^{39.44 \pm 0.04}$  to  $10^{39.50 \pm 0.07}$  erg s $^{-1}$  Mpc $^{-3}$  at  $z \simeq 0.2$  from our two previous LF best fits. The errors quoted here are the standard deviations taking into account that the three Schechter parameters are correlated, and so should be realistic estimates. Our value is 2.2 to 2.6 times higher than the value of Gallego et al. 1995 at  $z \sim 0$  ( $10^{39.09 \pm 0.04}$ , see Errata, 1996, ApJ, 459, L43). Consequently, our result shows that the star formation rate (SFR) is higher at  $z \simeq 0.2$  than that found in the local universe for galaxies with  $REW(H\alpha + [N II]) \gtrsim 10 \text{ \AA}$ . Figure 6 shows our data and the local measurements in the SFR vs.  $z$  plot from Madau et al. (1997) assuming a Salpeter (1955) IMF including stars in the mass range  $0.1 < M < 125 M_\odot$ . We used their conversion  $\mathcal{L}(H\alpha) = 10^{41.15} SFR/M_\odot \text{ yr}^{-1}$ , based on the stellar population synthesis models of Bruzual & Charlot (1997). The other points in this plot are from rest-frame UV continuum measurements. The comparison between the UV and H $\alpha$  results is not straightforward for the following reasons. As noted in the introduction, H $\alpha$  fluxes come from ionized gas surrounding OB stars, so are directly correlated to short-lived stars, once dust corrected with the Balmer decrement. The UV continuum comes from both short- and long-lived stars; the long-lived (late B, A0) stars contribute more to the UV continuum at larger UV wavelengths. In addition, Calzetti 1997 pointed that longer-lived non-ionizing stars are likely to be found in less obscured regions, than ionizing stars. This agrees with observations of starbursts where the extinction obtained with the Balmer decrement is found to be higher than the extinction obtained from UV continuum (Keel 1993). Given that UV photons are more obscured than H $\alpha$  photons, we expect that UV data should be less correlated to short-lived stars than H $\alpha$  data. Overall, converting H $\alpha$  luminosities to SFR depends less sensitively on the dust correction than on the assumed IMF. Converting UV luminosities to SFR depends less sensitively on IMFs in a standard cosmology (Baugh et al. 1997), than on uncertain dust extinction.

In Figure 6, the H $\alpha$  data are reddening corrected, while UV data are not, thus H $\alpha$  data must give higher values of star formation rate, than their counterpart in the UV. Calzetti et al. 1994 measured an *effective* dust extinction law from a sample of extended regions such as the central regions of starburst and blue compact galaxies. Their law is characterized by the absence of a 2175  $\text{\AA}$  dust feature. Assuming  $A_V = 1$  mag, it predicts an average dust extinction at 2000  $\text{\AA}$ , that is 1.95 times more in flux than at H $\alpha$ . Treyer et al. 1997 have a preliminary measurement of the UV(2000  $\text{\AA}$ ) density at  $z = 0.15$ , and find it is consistent with the UV(2800  $\text{\AA}$ ) CFRS data (Lilly et al. 1996). According to the results from Calzetti 1997, our Balmer decrement reddening of  $A_V = 1$  mag, would imply that the UV stellar continuum at 2000 and 2800  $\text{\AA}$  has an extinction of 1.3 and 1 mag respectively. Thus, our SFR result at  $\langle z \rangle = 0.2$  seems to be consistent with the UV(2000  $\text{\AA}$ ) data at  $\langle z \rangle = 0.15$ , and the UV(2800  $\text{\AA}$ ) data at  $\langle z \rangle = 0.35$  within the error bars.

### 4. Conclusion

We constructed an optically-selected H $\alpha$  luminosity function at  $z \simeq 0.2$ ; this will be useful as a comparison to future near-infrared spectroscopic surveys which will detect H $\alpha$  in galaxies near the expected peak of SFR. We find a total H $\alpha$  luminosity at least twice than the one measured in the local universe by Gallego et al. 1995 for galaxies with  $REW(H\alpha + [N II]) \gtrsim 10 \text{ \AA}$ . If the SFR evolution follows an  $(1+z)^3$  law, then  $\mathcal{L}(H\alpha)$  should decrease by a factor 1.7 from  $z = 0.2$  to  $z = 0$ . This factor is marginally outside the  $1 \sigma$  errors, and may suggest that the local H $\alpha$  density is low by  $\sim 20\%$ . This may correspond to the local under-density seen in optical redshift surveys (see Zucca et al. 1997). If the local estimate is correct then it implies an evolution proportional to  $(1+z)^{4.4}$ .

Since the number of hydrogen ionizing photons ( $\lambda < 912 \text{ \AA}$ ) emitted by a star is proportional to the H $\alpha$  recombination line, the total flux in H $\alpha$  is a good tracer of the number of ionizing stars within emission-line galaxies. The IMF introduces uncertainties in the relation between H $\alpha$  luminosity and star formation rate; H $\alpha$  traces only the massive, hot, short-lived stars, and therefore assumptions on the remaining fraction of cooler stars have to be made. Also, since star formation takes place in highly ob-

scured regions, newly formed stars are not detected in the UV or optical observations. Taking the SFR factor conversions from Madau (1997), our result is consistent with UV data corrected for  $\sim 1$  mag of dust extinction. Larger dust corrections would imply either an IMF with a shallower slope than the one from Salpeter, or an underestimation of the total  $H\alpha$  luminosity. However we are aware that uncertainties in models and in UV dust extinction are still large.

Another interesting result is the strong correlation observed between the flux emitted in the rest-frame  $B$ -band and  $H\alpha$  luminosity. Applying this relation to the CFRS where the rest-frame  $B$ -band is directly observed at  $z = 0.9$ , the range of sampled magnitudes suggests that all emission-line galaxies should be strong  $H\alpha$  emitters. This is in agreement with Hammer et al. 1997 who find an increase of the co-moving number of [O II] CFRS emitters by a factor at least 5 up to  $z \sim 1$ . This correlates with the evolution seen in the CFRS LFs, which is due to these bright, star-forming galaxies. At high redshifts, deep spectroscopic surveys clearly become biased toward strong emission-line, dust-free emitters, which contribute to the increase of the total luminosity of these galaxies at earlier epochs, however they may be only the tip of the iceberg of all  $H\alpha$  emitters.

It is a pleasure for LT to thank her colleagues David Crampton, François Hammer, Olivier Le Fèvre and Simon Lilly, who made the CFRS survey possible. This work has benefited from fruitful discussions with Stéphane Charlot. We thank Piero Madau, who kindly provided his most recent SFR conversion factors. LT acknowledges support from the European HCM program/ERBCHBICT941612. SJM acknowledges support from a PPARC advanced fellowship.

## REFERENCES

Baugh, C. M., Cole, S., Frenk, C. S., Lacey, C. G. 1997, *AJ*, in press (astro-ph/9703111)

Bruzual, G., & Charlot, S. 1997, in preparation

Calzetti, D., Kinney, A. L., Storchi-Bergmann, T. 1994, *ApJ*, 429, 582

Calzetti D. 1997, Proceedings of the conference “The Ultraviolet Universe at Low and High Redshift” (2-4 May 97), AIP press, ed. W. Waller, in press (astro-ph/9706121)

Crampton D., Le Fèvre, O., Lilly, S. J., Hammer, F. 1995, *ApJ*, 455, 96

Ellis, R.S., Colless, M., Broadhurst, T. J., Heyl, J., Glazebrook, K. 1996, *MNRAS*, 280, 235

Gallego, J., Zamorano, J., Rego, M., Vitores, A. G. 1997, *ApJ*, 475, 502

Gallego, J., Zamorano, J., Aragón-Salamanca, A., Rego, M., 1995, *ApJ*, 455, L1

Hammer, F., Flores, H., Lilly, S. J., Crampton, D., Le Fèvre, O., Rola, C., Mallen-Ornelas, G., Schade, D., Tresse, L. 1997, *ApJ*, 481, 49

Keel, W. C. 1993, in *Massive Stars: Their lives in the Interstellar Medium*, ed. J. P. Cassinelli & E. B. Churchwell (ASP Conf. Series, 35), 498.

Kennicutt, R. C., Kent, S. M. 1983, *ApJ*, 88, 1094

Kennicutt, R. C. 1992, *ApJ*, 388, 310

Le Fèvre, O., Crampton, D., Lilly, S.J., Hammer, F., Tresse, L. 1995, *ApJ*, 455, 60

Lilly, S. J., Le Fèvre, O., Crampton, D., Hammer, F., Tresse, L. 1995a, *ApJ*, 455, 50

Lilly, S. J., Tresse, L., Hammer, F., Crampton, D., Le Fèvre, O., 1995c, *ApJ*, 455, 108

Lilly, S. J., Le Fèvre, O., Hammer, F., Crampton, D. 1996, *ApJ*, 460, L1

Madau, P., Ferguson, H. C., Dickinson, M. E., Giavalisco, M., Steidel, C. C., Fruchter, A. 1996, *MNRAS*, 283, 1388

Madau, P., Pozzetti, L., Dickinson, M. E. 1997, *ApJ*, submitted

Osterbrock, D. E. 1989, *Astrophysics of Gaseous Nebulae and Active Galactic Nuclei*, Univ. Sci. Books

Salpeter, E. E., 1955, *ApJ*, 121, 61

Sarajedini V. L., Green R. F., Griffiths R. E., Ratnatunga K. 1996, *ApJ*, 471, L15

Schechter, P., 1976, *ApJ*, 203, 297

Seaton, M. J., 1979, *MNRAS*, 187, 73

Steidel, C. C., Giavalisco, M., Pettini, M., Dickinson, M., Adelberger, K. L., 1996a, *ApJ*, 462, L17

Tresse, L., Rola, C., Hammer, F., Stasińska, G., Le Fèvre, O., Lilly, S. J., Crampton, D. 1996, MNRAS, 281, 847 (CFRS-XII)

Tresse, L., Maddox, S. J., Loveday, J. 1998, MNRAS, in preparation

Treyer, M. A., Ellis, R. S., Milliard, B., Donas, J. 1997, Proceedings of the conference “The Ultraviolet Universe at Low and High Redshift” (2-4 May 97), AIP press, ed. W. Waller, in press (astro-ph/9706223)

Zucca, E., Zamorani, G., Vettolani, G., Cappi, A., Merighi, R., Mignoli, M., Stirpe, G. M., MacGillivray, H., Collins, C., Balkowski, C., Cayatte, V., Maurogordato, S., Proust, D., Chincarini, G., Guzzo, L., Maccagni, D., Scaramella, R., Blanchard, A., Ramella, M. 1997, A&A, in press (astro-ph/9705096)



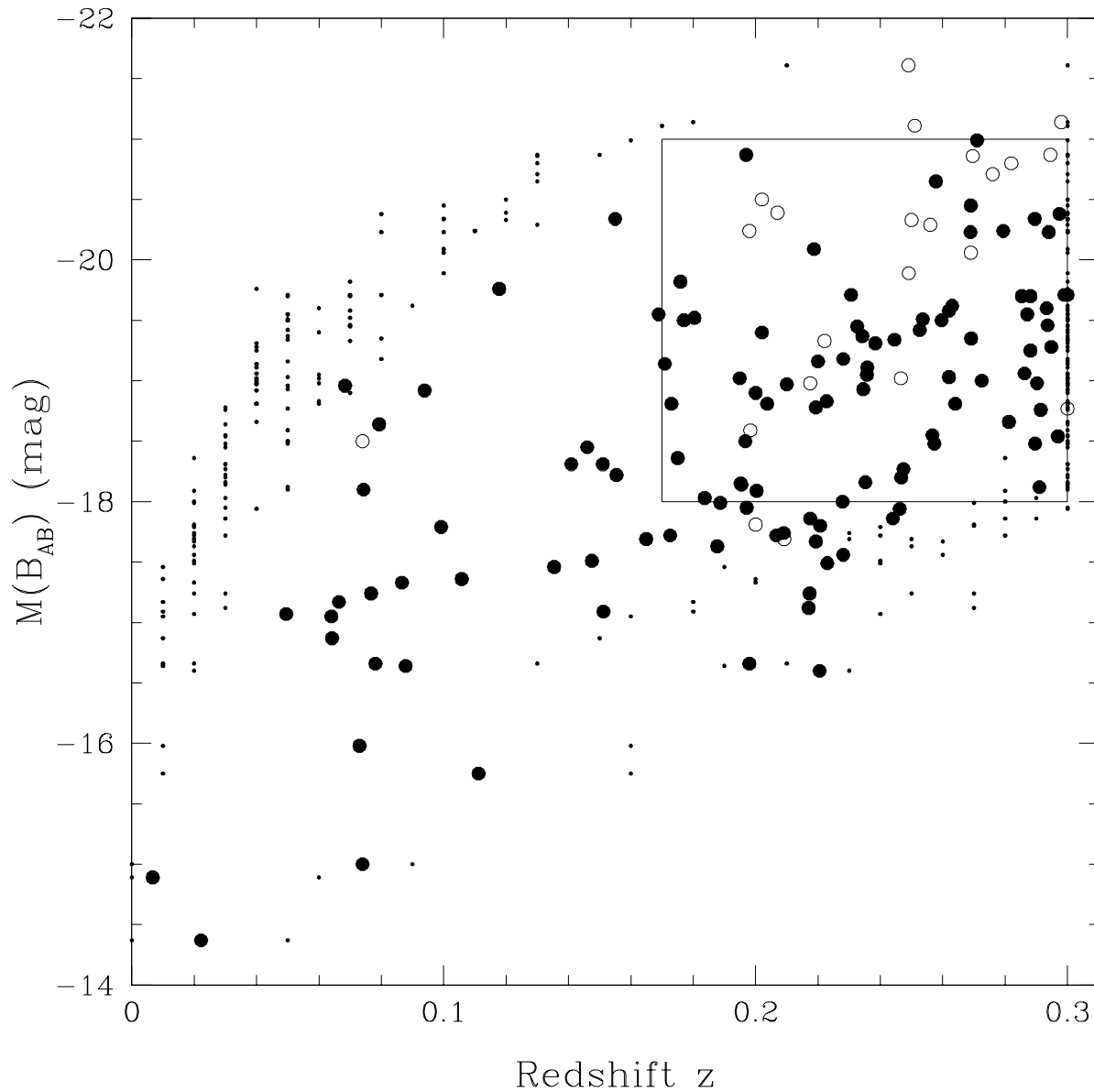


Fig. 1.— Absolute magnitudes in  $B_{AB}$  versus redshift  $z$  of the 138 CFRS galaxies at  $z \leq 0.3$ . The filled circles represent  $H\alpha$  emitting galaxies, the open circles show  $H\alpha$  absorbing galaxies. The small dots are the minimal and maximal redshifts in which a galaxy could be detected as used in the  $V_{max}$  method (see text). The rectangle shows an homogeneous subsample of galaxies at  $0.17 < z < 0.3$  and  $-21 < M(B_{AB}) < -18$ .

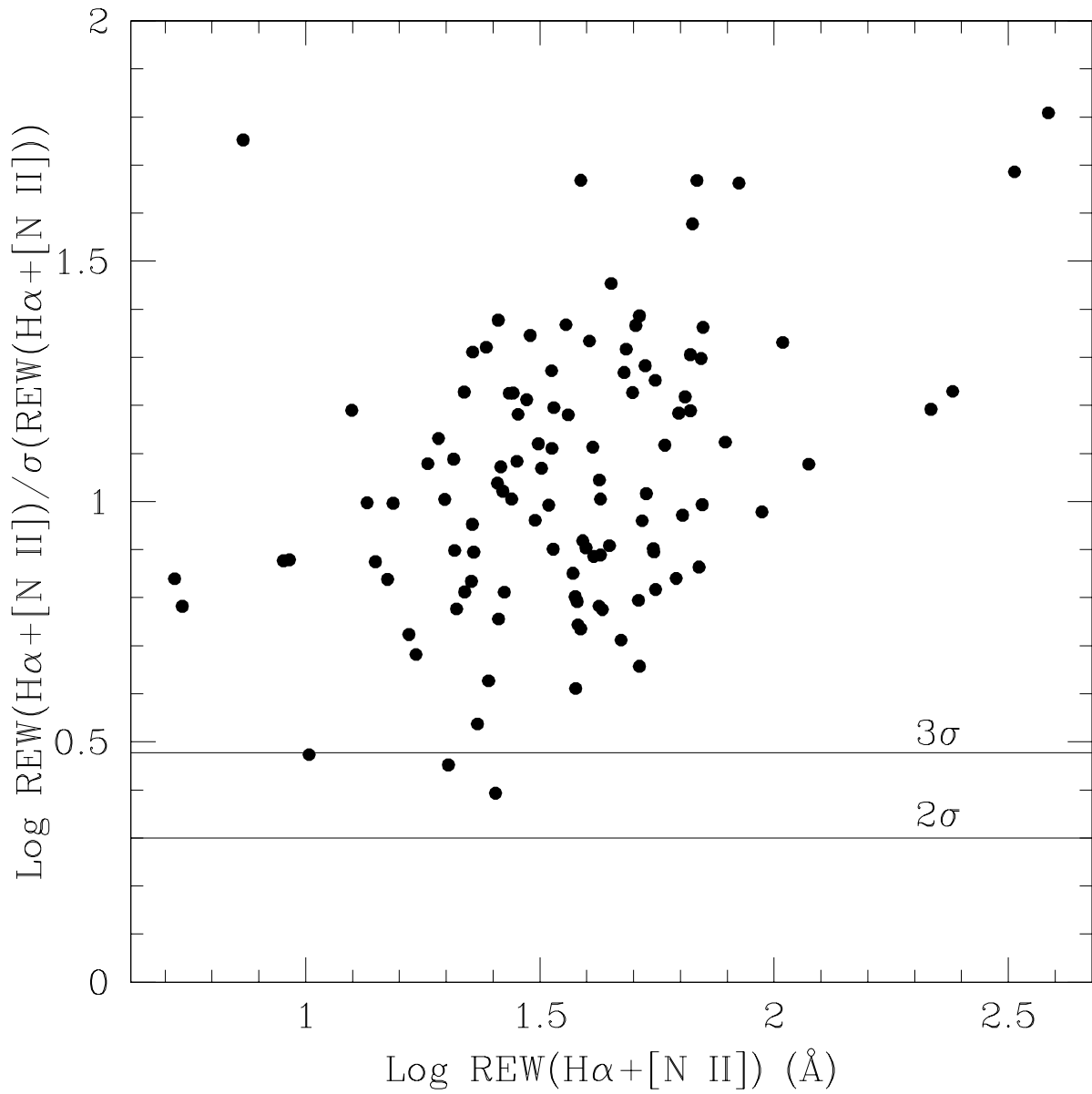


Fig. 2.— Detection level of  $\text{REW(H}\alpha\text{+[N II])}$  versus  $\text{REW(H}\alpha\text{+[N II])}$ .

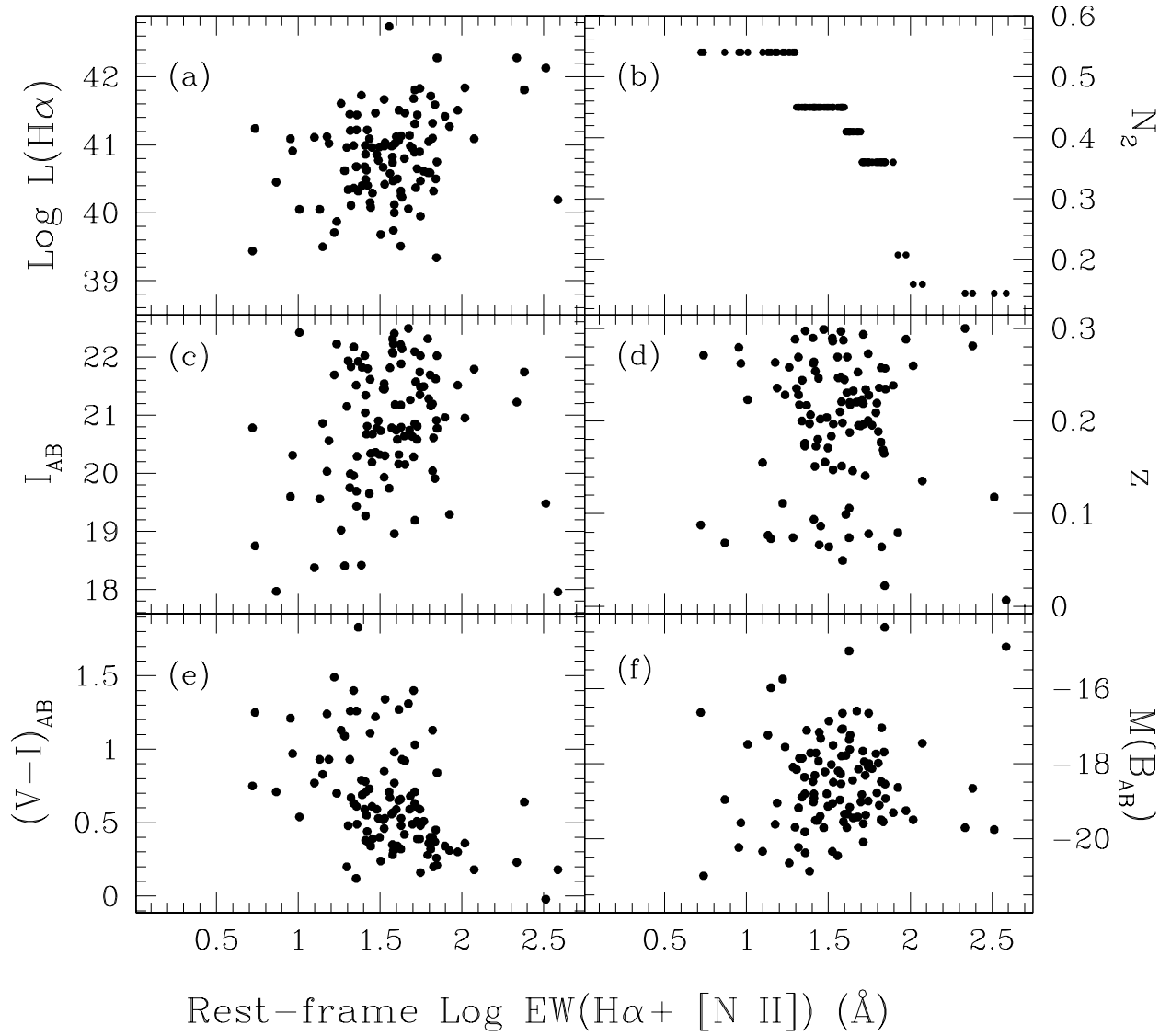


Fig. 3.— Relations between REW(H $\alpha$ + [N II]) and other parameters as labeled. They are useful to compare our sample with other emission-line surveys.

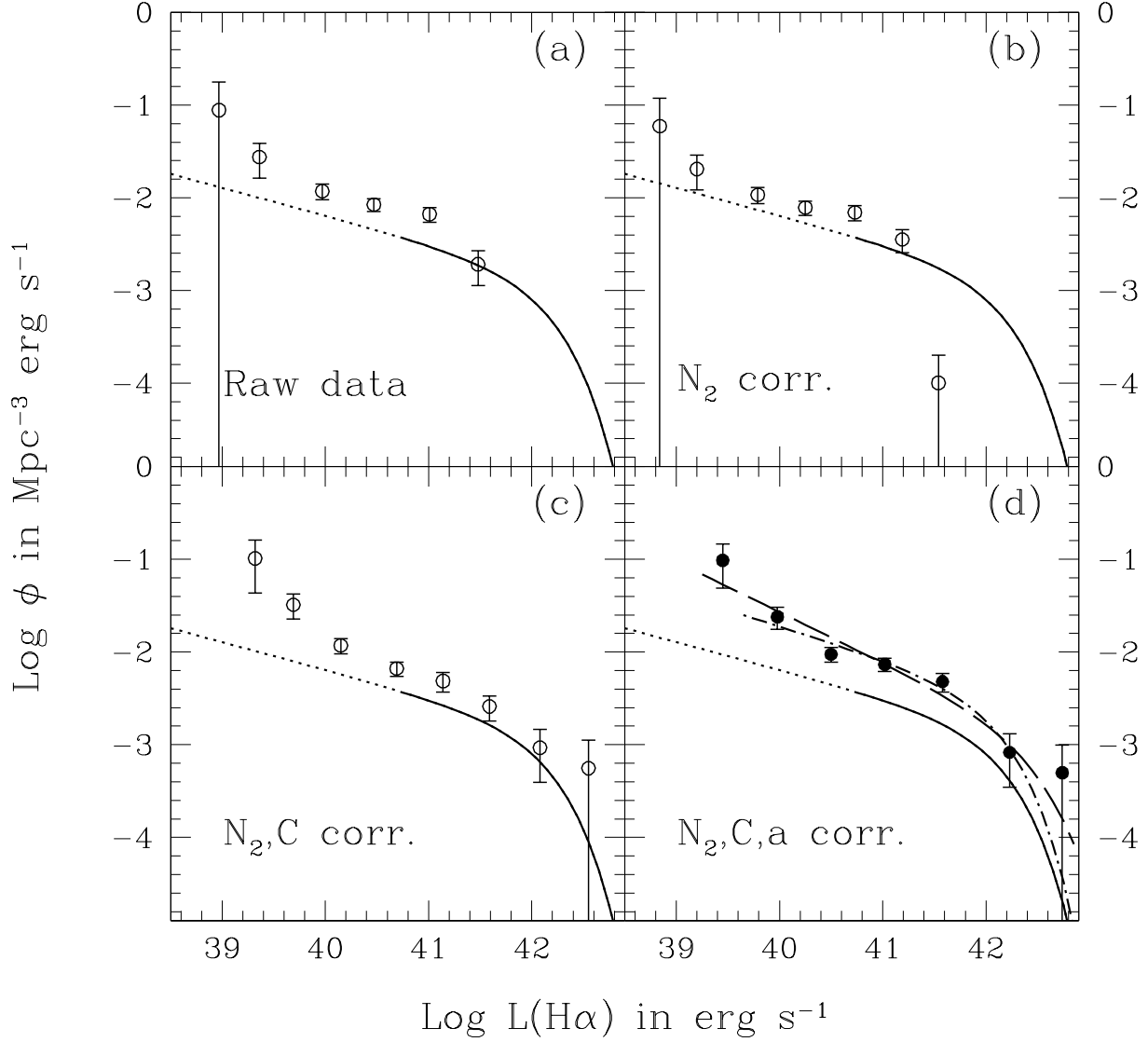


Fig. 4.— Overall  $H\alpha$  luminosity function at  $z \leq 0.3$ . The LFs with open circles show the successive corrections to obtain the final LF shown by the filled circles in panel (d). The raw data are shown in panel (a). Panel (b) shows this after correcting for the  $[N \text{ II}]$  contribution to  $H\alpha$  ( $N_2$ ). Panel (c) is further corrected for the reddening  $C$ . Applying the aperture correction  $a$  gives the final LF in panel (d). In each plot, the solid curve is the Gallego et al. 1996  $H\alpha$  LF at  $z \simeq 0$ , the dotted curve is its extension to fainter luminosities. The long-dashed and dot-dashed curves are the best Schechter (1976) fits to our data, the latter one is given by excluding the faintest bin.

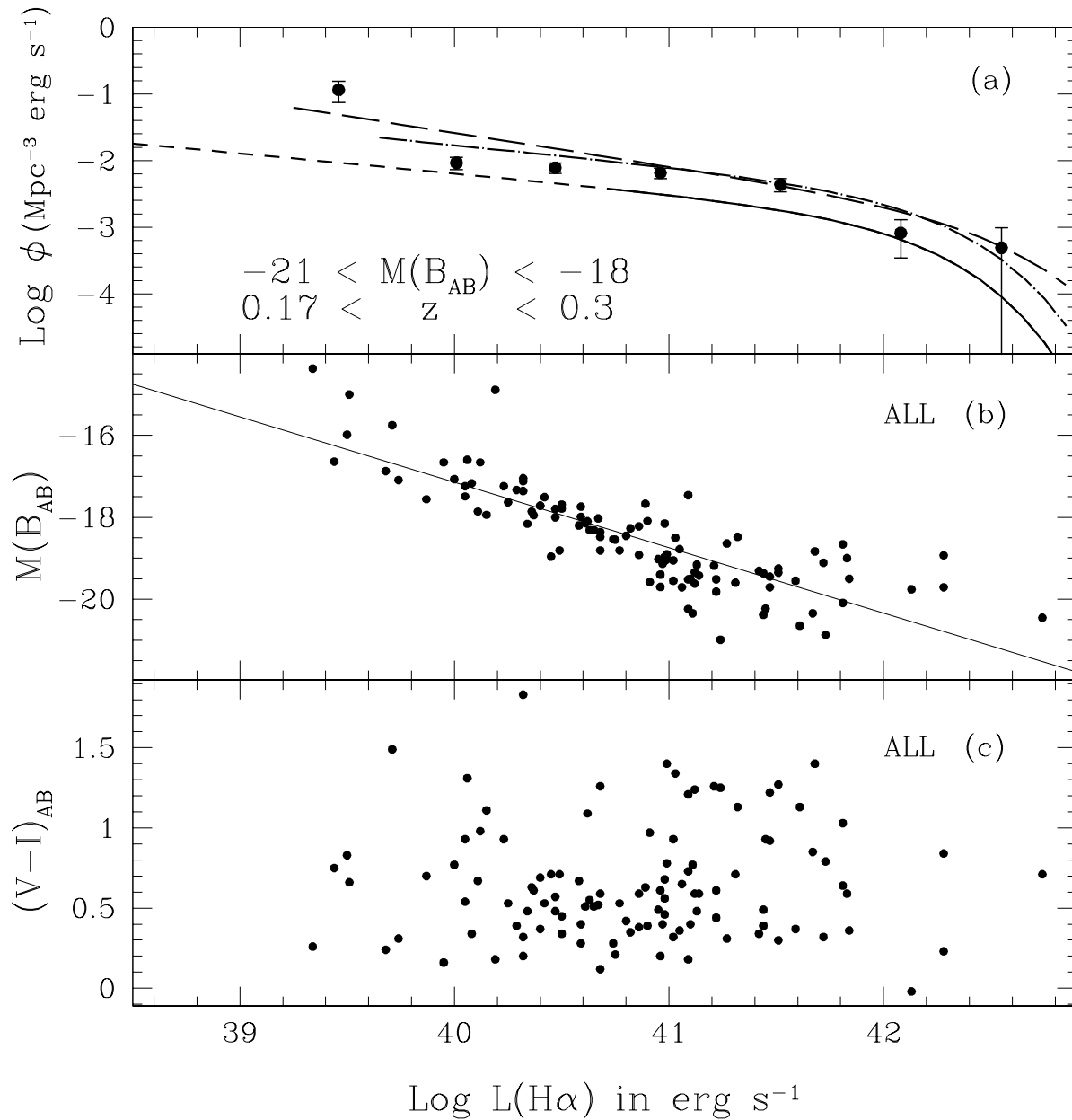


Fig. 5.— The panel (a) shows the  $\text{H}\alpha$  LF of the data within the rectangle shown in Figure 1. The curves are the same as in Figure 4d. The panels (b) and (c) show  $M(B_{AB})$  and  $(V-I)_{AB}$  versus  $\text{H}\alpha$  luminosities of all the  $\text{H}\alpha$  emitters. Galaxies redder than a local Sb spiral have  $(V-I)_{AB} \gtrsim 0.7$  at  $z < 0.3$ .

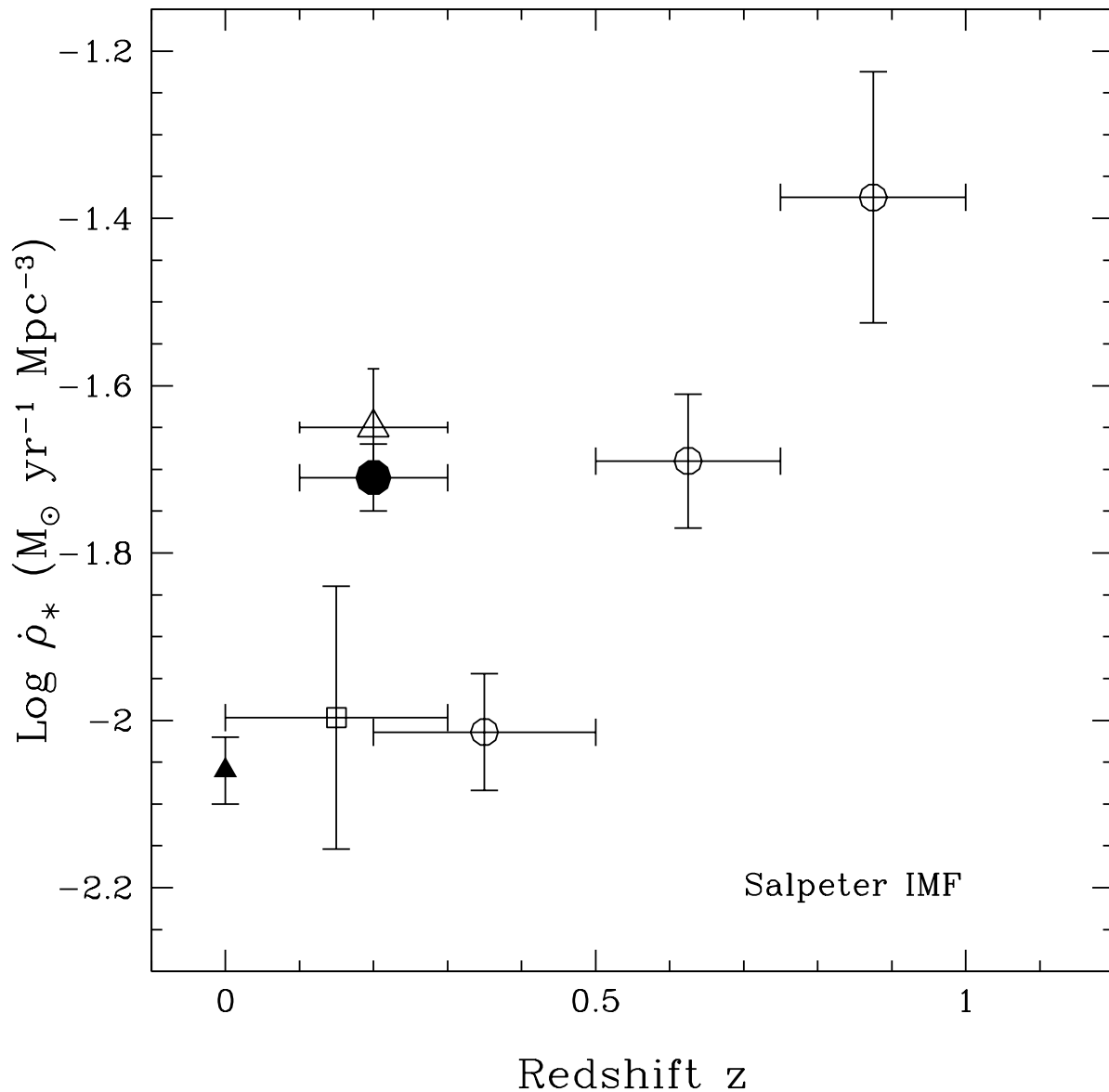


Fig. 6.— Comoving volume-averaged star formation rate versus redshift. The open circles are from the “LF-estimated” UV(2800 Å) CFRS data of Lilly et al. 1996, the open square is from UV(2000 Å) data of Treyer et al. 1997, and the filled triangle is from H $\alpha$  data of Gallego et al. 1995. The filled circle is our H $\alpha$  result (the open star is our result if the faintest bin of our H $\alpha$  LF is included.) We used the Madau et al. (1997) conversion factors;  $\log \mathcal{L}(H\alpha) = 41.15 + \log \dot{\rho}_*$ , and  $\log \mathcal{L}_{UV} = 27.9 + \log \dot{\rho}_*$ , assuming a Salpeter IMF and including stars in the  $0.1 - 125 M_\odot$  mass range.